The Effect Of Deposition Time On The Microstructure And Resistivity Of Cu/Ni Thin Film Prepared By Magnetized Electroplating

Muthi'ah Lutfia Khansa, Moh. Toifur, Guntur Maruto, Yudhiakto Pramudya, Azmi Khusnani

Abstract: Thin films of Cu/Ni have been synthesized by the electroplating method assisted by a magnetic field on the variation of deposition time. The purpose of this paper was to investigate the dependence of sheets resistivity on microstructure obtained through XRD and SEM-EDX tests. Cu plates are used as cathodes and Ni plates as anodes. The electroplating process is carried out at DC voltage of 1.5 volt, 200 gauss magnetic field, 60° C solution temperature, and 4 cm electrode distance. Electrolyte solutions are made from a mixture of H_3BO_3 (30 g), $NiCl_2$ (195 g), $NiSO_4$ (45 g), and H_2O (750 ml). Deposition times varied from 5 s–45 s with intervals of 10 s. Based on the results of the microstructure test using XRD, all samples have a crystalline structure with intensity, d-spacing and grain size that varies with the time of deposition. From the EDS analysis, it is known that Ni deposit levels increase with increasing deposition time. The sheet resistivity range from $(4.87 \pm 0.02)\times10^{-3}$ Ω/sq to $(1.38 \pm 0.06) \times10^{-3}$ Ω/sq.

Index Terms: Cu/Ni thin film, electroplating, deposition time, sheet resistivity, microstructure.

1 INTRODUCTION

Iinstrumentation in cryogenic conditions involves extreme temperatures so that conventional measuring equipment cannot be used. One type of sensor used to measure low temperatures is a Resistance Temperature Detector (RTD). RTD is a material that has temperature-dependent resistivity [1]. The metal commonly used for RTD is platinum (Pt), because it has a high TCR (temperature coefficient of resistance) [2,3] other more inexpensive materials are copper (Cu) and nickel (Ni) [4,5,6]. Copper and nickel can be used as low-temperature sensor materials because they can measure temperatures from 38.5 K to 673 K. As a low-temperature sensor, copper and nickel can be made into thin layers by depositing Ni in Cu using the electroplating method [6]. The advantage of the electroplating method is that the process temperature is quite low, the process can be carried out at atmospheric pressure, simple equipment, fast sedimentation rate, porosity in the layer is relatively low and can produce several layers [7]. To obtain good coating results, there are several influential parameters, namely electrolyte concentration, acidity (pH), current density, temperature, agitation, and settling time [8,9]. To improve the quality of deposition results, some researchers added magnetic fields to the electroplating process. Adding a magnetic field in a direction perpendicular to the electric current will generate the Lorentz force. The interaction between the Lorentz force and Ni ions will increase deposit mass transport [10,11] and reduce the reaction effect of hydrogen evolution [12,13]. Addition of magnetic field to the process of making thin layers can make thin layers more homogeneous [14,15].

- *Muthi'ah Lutfia Khansa is currently pursuing masters degree program in Physics Education in Ahmad Dahlan University, Indonesia. E-mail: mutiakhansa@gmail.com*
- *Moh Toifur is currently a Physics lecturer in Ahmad Dahlan University, Indonesia. E-mail: mtoifur@yahoo.com*
- *Guntur Maruto is currently a Physics lecturer in Gadjah Mada University, Indonesia.*
- *Yudhiakto Pramudya is currently a Physics lecturer in Ahmad Dahlan University, Indonesia. E-mail: ypramudya@gmail.com*
- *Azmi Khusnani is currently pursuing masters degree program in Physics Education in Ahmad Dahlan University, Indonesia. E-mail: husnaniazmi@gmail.com*

In this study, the thin layer Cu/Ni was synthesized by the electroplating method assisted by magnetic fields at various deposition times from 5 to 45 s. Deposition time - as stated in Faraday's law - has a linear effect on the thickness of the formed layer [16,17]. The longer the electroplating process, the greater the accumulation of electron movement and material transfer in the area between the two electrodes. Addition of layer deposits affects changes in resistivity. Changes in resistivity will correlate with the sensitivity of the Cu/Ni thin layer when used as a sensor material [18].

2 EXPERIMENTAL PROCEDURE

The material used in this research is copper (Cu) plate as a substrate with the size of 2.5 cm × 1.0 cm × 0.02 cm and nickel (Ni) with the size of 3 cm × 1.0 cm × 0.4 cm as a coated material. The copper plate is polished with autosol, then cleaned with toothpaste and rinsed with 60° C distilled water gradually three times. The copper plate is rinsed with 96% alcohol in an ultrasonic cleaner for 3 minutes. The sample is dried and stored in the dry box. The electrolyte solution made from a mixture of nickel sulfate ($NiSO_4$), nickel chloride ($NiCl_2$), boric acid (H_3BO_3), and distilled water of 195 g, 45 g, 30 g, 750 ml, respectively. Electrolyte solutions are stirred in a beaker glass using a magnetic stirrer for 4 hours. Then poured in plat bath — the tool design as in Fig. 1 the magnetic field to be set at 200 gauss. The electroplating process is carried out at DC voltage of 1.5 volt, 60° C solution temperature, and 4 cm electrode distance. Deposition times varied from 5 s – 45 s with intervals of 10 s. Characterization of Cu / Ni layers was carried out by microstructure test with SEM-EDX, XRD, and sheet resistivity with a four-point probe. From SEM image, it can be seen the surface condition of the sample at each variation of deposition time. EDX analysis was carried out to determine the Cu and Ni content in each sample.

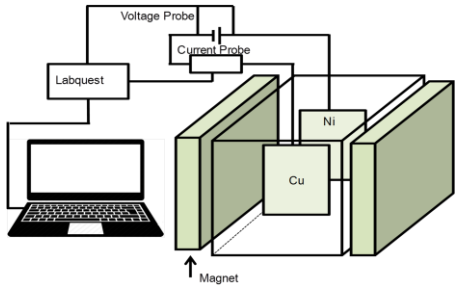

***Fig. 1**. M Schematic diagram of the experimental setup*

The XRD test was used to determine the structure and regularity of the formed Ni crystals. Scherrer formula is used to obtain grain size. Resistivity test is carried out to determine the relationship between sheet resistivity and microstructure. To determine the sheet resistivity a voltage-current data fitting is performed (Vi, Ii) following a linear equation. If the curve slope is a, then,

$$R_s = \frac{\pi}{\ln 2}\frac{V}{I} = \frac{\pi}{\ln 2}a \qquad (1)$$

3 RESULT AND DISCUSSION

In Figure 2, SEM images of the surface of the Cu / Ni layer deposited on the deposition time variation are presented.

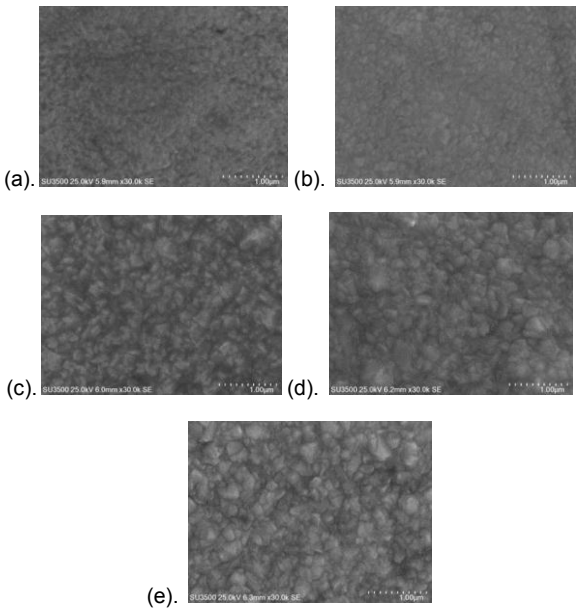

***Fig. 2**. SEM images with 30,000x magnification for variations in deposition time (a) 5 s, (b) 15 s, (c) 25 s, (d) 35 s, (e) 45 s.*

Based on Figure 2, information can be obtained that each sample has a different morphological appearance. The longer the deposition time, the larger the grain size. In figure 2 (a) the layer is still very thin, then the layer becomes thicker at the time of deposition 15 s as in figure 2 (b). Then figure 2 (c) granules with relatively uniform size are formed. In figure 2 (d) in various places the grain size is larger than the average size. While in Figure 2 (e) it appears that the increase in thickness of the layer is able to make granules that were not homogeneous before becoming more homogeneous. Furthermore, to determine the quantity of Cu and Ni in the sample in figure 3 a graph of the percentage of Cu and Ni mass at various deposition times is presented. Data graph is obtained from the EDS spectrum. As time increases the percentage deposition of Ni mass increases [16,19]. Depositions for 45s have been able to increase Ni content from 21% for deposition for 5s to 88% or an increase of 67%. This shows that the Ni deposit is thicker with the addition of deposition time. The equation that states the relationship between deposition time (t) and mass percentage Ni (W) is

$$W = 1.7364t + 15.102 \qquad (2)$$

with an index of determination R^2 = 0.97. With the R^2 value, the deposition time is strong enough to determine the percentage of Ni mass formed on the Cu substrate.

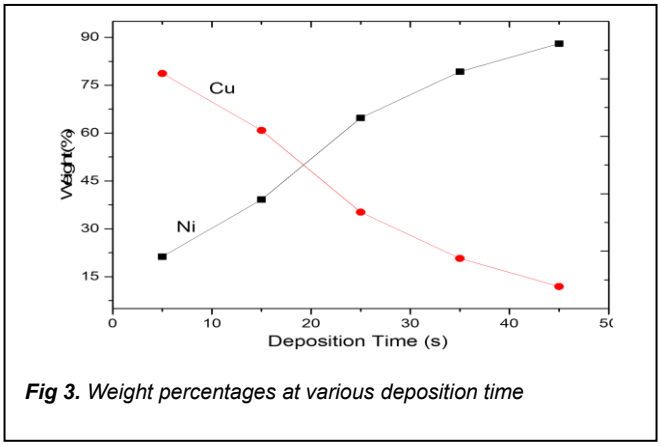

***Fig 3.** Weight percentages at various deposition time*

In Figure 4, a diffractogram of the Cu / Ni layer is shown in the variation in deposition time. Based on the picture, it is known that all samples have a crystal structure except for samples from Ni deposition for 5 s. The Ni peak is at ±45° diffraction angle in direction (111). From the observation of the position of the diffraction peak angle, it turns out that deposition time affects the position of the diffraction peak angle (as shown on the subgraph) which tends to shift more to the left. This diffraction peak angle shift affects the distance between the crystal fields. Furthermore, in deposition samples within 5 s, the diffraction peaks did not appear. If this is confirmed by the EDS data the actual Ni layer exists because there is a mass percent of Ni of 21%. So it was concluded that in this sample the Ni layer had an amorphous structure.

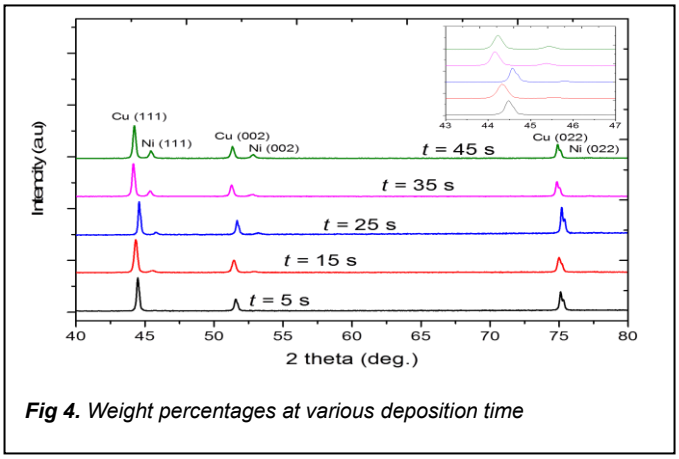

***Fig 4.** Weight percentages at various deposition time*

Furthermore, in Figure 5, the X-ray diffraction peak intensity curve is displayed on the variation in deposition time.

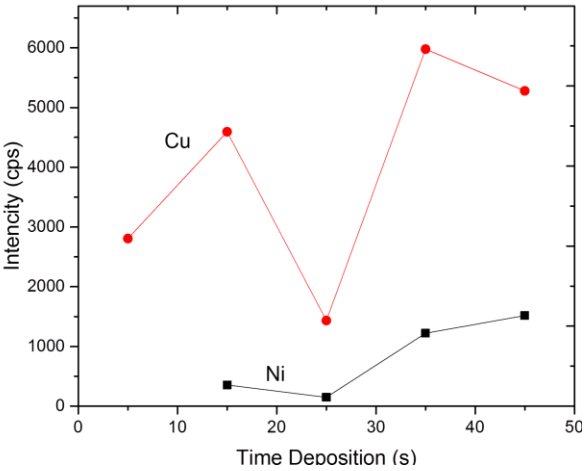

Fig 5. *The diffraction intensity of Cu and Ni at various deposition time*

When observed in Figure 5, the intensity of Ni is not linearly related to the time of deposition but there is a tendency to increase. This can be seen in the deposition 15 s when Ni peaks appeared with an intensity of 355 cps, while at 25 s the intensity values decreased by 208 cps and the intensity values rose again at the time of deposition 35 s and 45 s. The decrease in the value of Ni intensity at deposition time 25s can be caused because the Cu substrate used is not good, this can be seen in the intensity of Cu which has the smallest value compared to the others. Based on this, it is estimated that the surface conditions of the substrate are uneven so that the layers grown on it are uneven [20]. Changes in diffraction angle cause changes in interplanar distance. From the Bragg diffraction formula if the diffraction angle shifts to the right, the interplanar distance becomes smaller. Likewise, from the Scherrer formula, the shift in the diffraction angle to the right causes the size of the particle to become larger. In Figure 6a the interplanar distance of Cu and Ni is shown, where d-spacing in Cu and Ni is parallel to each other. This shows that the formation of Ni atoms in the Cu / Ni layer follows the formation of Cu atoms. Because the size of Ni atoms is greater than the size of Cu atoms (radius of Ni atom 1.91 and radius of Cu atom 1.90), the interplanar Ni distance is smaller than interplanar Cu distance. The decrease in d-spacing for deposition samples at 25 s if confirmed by a small (less regular) diffraction intensity curve shows the number of crystal defects in the sample. This crystal defect can be in the form of an interstate (filling outside the atomic lattice). Similarly, this happened for deposition at the time of 45 s. But the intertition particle content is not as much as the deposition sample at 25 s. In Figure 6b, the grain size of Cu and Ni is displayed at various deposition times.

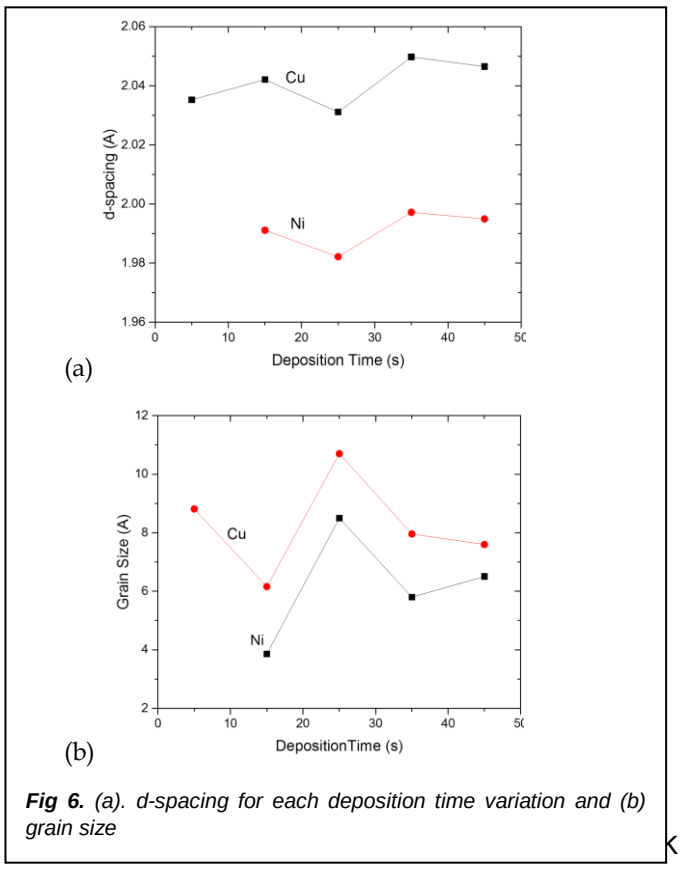

Fig 6. *(a). d-spacing for each deposition time variation and (b) grain size*

K

Cu X-rays, with λ= 1.5419 Å. The value of grain size depends on two things, namely the diffraction angle and FWHM. From the figure 6, it appears that deposition samples within 25 s have the highest grain size compared to the other samples. This is due to a large number of intertition resulting in larger grains. In Figure 7 is shown the sheet resistivity of Cu and Cu/Ni. From the figure, it appears that the sheet resistivity of Cu increases after being deposited with Ni. In line with the increase in deposition time, the sheet resisitivity of Cu/Ni become decrease. The curvature of the curves for Rs-Cu and Rs-Cu/Ni shows that the five Cu substrate used has different Rs. This affects the value of Rs-Cu/Ni.

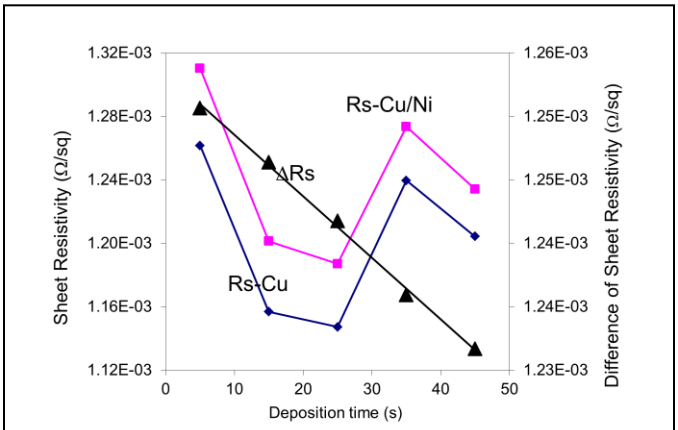

Fig 7. *The sheet resistivity of Cu and Cu/Ni*

The value of resistivity depends on the grain size, intensity, and interplanar distance. The value of Rs is inversely proportional to the grain size Ni (Rs ~ 1 / grain size) [21], inversely proportional to the diffraction intensity, and proportional to the interplanar distance. There are samples whose interplanar distances dominate Rs and conversely, the grain size dominates the value of Rs. From Figure 7 it appears that the value of Rs Cu / Ni is very dependent on the value of Rs Cu. The value of Rs Cu depends on the microstructure of the Cu surface. In deposition samples at the time of 5 s, because the amorphous layer is formed, the resistivity becomes the highest of 1.31×10^{-3} Ω/sq. Furthermore, in deposition samples within 15 s a decrease of up to 1.2×10^{-3} Ω/sq. This value is quite low among the other Rs values. This is caused by small d-spacing so that the electric current becomes easy to pass through. The small grain size and the intensity of the small diffraction peak are not able to compensate for the small d-spacing so that the Rs are small. For deposition samples at the time of 25 s, Rs is 1.19×10^{-3} Ω/sq. This value is the smallest among the other Rs values. The small Rs is because the grain is large at 8.50 Å, while the intensity and d-spacing are small even though it can increase the value of Rs but have not been able to compensate for Rs due to the size of the grain size. Furthermore, for deposition samples within 35s obtained Rs 1.27×10^{-3} Ω/sq. This value is the highest among the other Rs. The amount of Rs is contributed by a large d-spacing, a small grain size of 5.80 Å. The crystal structure of Ni in this sample is quite good so that it can reduce Rs, but the reduction in Rs due to the regularity of the crystal structure has not been able to compensate for Rs derived from d-spacing and grain size. Furthermore, for deposition samples at 45 s obtained Rs of 1.23×10^{-3}Ω/sq. This value is below the Rs of the deposited sample within 25 s. Rs is contributed by d-spacing and a small grain size. While the crystal structure of the sample is very good. Various changes in intensity, d-spacing, and grain size concerning actual deposition time are caused not only by Ni deposition but also by the condition of the Cu substrate. This can be seen in the similarity of the profiles of the Cu curves for the three variables. However, we can determine the effect of deposition time on changes in Rs through the difference in Rs before Ni is coated and after Ni coated. The value as shown in figure 7 concerning ΔRs. From this graph, it appears to be a straight line that goes down with the equation

$$\Delta R_s = -4.8\times10^{-7}t + 0.0013\,(\Omega/\mathrm{sq}) \quad (3)$$

With a determination index is 0.99. With this R^2, a strong proportional relation between deposition time and an increase in Rs is obtained. This means that the increase in Rs layer is proportional to the time of deposition of Ni.

4 CONCLUSION

Based on the data analysis, the results of the study show that deposition time affects the microstructure of Cu/Ni layers. The deposition of Ni with a time of 5 s has not formed a crystal structure, so it is better to do the deposition process in more than 5 s. The surface condition of the Cu substrate affects the Ni layer that grows on it. The sheet resistivity is influenced by the microstructure of the Cu/Ni layer. The diffraction intensity is inversely proportional to Rs, grain size is inversely proportional to Rs, and d-spacing is directly proportional to Rs.

5 ACKNOWLEDGMENT

This research is the preliminary research from the main research concerning with Cu/Ni temperature sensor. This research is funded by the Ministry of Research Technology and the Higher Education Republic of Indonesia through The 2019 Post Graduate Research Grant Year (PTM) Scheme with Contract No PTM-022/SKPP.TT/LPPM UAD/III/2019.

6 REFERENCES

[1] T. Chowdhury, and H. Bulbul, “Design of a Temperature Sensitive Voltage Regulator for AC Load Using RTD,” International Journal of Engineering Science and Technology, 12 (2) 7896-7903. 2010.

[2] S. K. Sen, T.K. Pan, and P. Ghosal, “An Improved Lead Wire Compensation Technique for Conventional Four Wire Resistance Temperature Detectors (RTDs),” Measurement, 44 (2011) 842-846. 2011.

[3] Maher, V. Velusamy, D. Riordan, and J. Walsh,” Modelling of Temperature Coefficient of Resistance Of A Thin Film RTD Towards Exhaust Gas Measurement Applications,” Proceedings of the 8th International Conference on Sensing Technology, 19–22. 2014.

[4] J. Fraden, Handbook of Modern Sensors: Physics, Designs, and Applications, New York: Springer. 2003.

[5] R. L. Boylestad, Introductory Circuit Analysis, Twelfth Edition, United States of America: Parential Hall Pearson. 2014.

[6] M. Toifur, Y. Yuningsih, A. Khusnani, “Microstructure, thickness and sheet resistivity of Cu/Ni thin film produced by Electroplating Technique on the Variation of Electrolyte Temperature,” IOP Conf. Series: Journal of Physics: Conf. Series 997 012053. 2018

[7] N.N. Le, T.C.H. Phan, A. D. Le, T.M..Y. Dang, and M.C. Dang, “Optimization of copper electroplating process applied for microfabrication on flexible polyethylene terephthalate substrate,” Adv. Nat. Sci.: Nanosci. Nanotechnol, 035007 (6pp). 2015.

[8] K. Seshan, “Handbook of Thin-Film Deposition Processes and Techniques - Principles, Methods, Equipment and Applications (2nd Edition) Chapter 8 Sputtering and Sputter Deposition,” https://doi.org/10.1002/ange.198910 10662 . 2002.

[9] S .E. Guler, Karakaya, E. Konca, “Effects Of Current Density, Coating Thickness, Temperature, Ph And Particle Concentration On Internal Stress During Ni–Mos2 Electrocodeposition,” Surface Engineering, Vol 30, No.2, (2014), pp. 109-114. 2014.

[10] V. Ganesh, D. Vijayaraghavan, and V. Lakshminarayanan, “Fine Grain Growth oNickel Electrodeposit: Effect of Applied Magnetic Feld During Deposition,” Applied Surface Science, 240(1–4), 286–295. 2005.

[11] M. Ebadi, W..J. Basirun, and Y. Alias, “Influence of Magnetic Field on The Electrodeposition of Ni–Co Alloy,” Journal of Chemical Sciences, 122(2), 279–285. 2010.

[12] M. Zielinsky, E. Miękoś, D. Szczukocki, R. Dałkowski, A. Leniart, B. Krawczyk and R. Juszczak, “Effects of Constant Magnetic Field on Electrodeposition of CoW-Cu Alloy,” International Journal of Electrochemical Science Volume 10, Issue 5, pp. 4146- 4154. 2015.

[13] K. Kołodziejczyk, E. Miękoś, M. Zieliński, M. Jaksender, D. Szczukocki, K. Czarny and B. Krawczyk, ”Influence Of Constant Magnetic Field On Electrodeposition Of Metals,

Alloys, Conductive Polymers, And Organic Reactions," Journal of Solid State Electrochemistry, 1629–1647. 2017.
[14] Y.D. Yu, Z.L. Song, H.L. Ge, and G.Y. Wei, "Influence Of Magnetic Fields On Cobalt Electrodeposition," Surface Engineering, 30(2), 83–86. 2014.
[15] L.M. Monzon and J.M. Coey, "Magnetic Felds in Electrochemistry: The Kelvin Force. A Mini-Review," Electrochemistry Communications, (42), 38-41. 2014
[16] T.J. Tuaweri, E.M. Adigio, and P.P. Jombo, "A Study Of Paremeters Zinc Electrodeposition from a Sulphate Bath," International Journal of Engineering Science Invention, ISSN 2319-6726. P. 17-24. 2013.
[17] S. Kumar, S. Pande, and P.Verma, "Factor Effecting Electro-Deposition Process," International Journal of Current Engineering and Technology, Vol 5 No 2. 2015.
[18] N. Afsarimanesh, A.P. Zaheer, "LabVIEW Based Characterization and Optimization of Thermal Sensors," International Journal on Smart Sensing and Intelligent Systems, Vol. 4 No. 4, pp. 726-739. 2011
[19] D.H. Jung, A. Sharma, K.H. Kim, Y.C. Choo, J.P. Jung, " Effect of Current Density and Plating Time on Cu Electroplating in TSV and Low Alpha Solder Bumping," Journal of Materials Engineering and Performance, 1059-9495. 2015.
[20] M. Schlesinger, P. Ivan, "Modern Electroplating, 5th Edition," New Jersey: Wiley. 2014.
[21] M. Apreutesei, C. Lopez, J.Borges, F. Vaz, and F. Macedo, "Modulated IR Radiometry For Determining Thermal Properties And Basic Characteristics Of Titanium Thin Films Modulated IR Radiometry For Determining Thermal Properties And Basic Characteristics Of Titanium Thin Films," J. Vac. Sci, Technol. A, 32(4). 2014.